

Observations of X-Ray Jets with the Yohkoh Soft X-Ray Telescope

Kazunari SHIBATA,¹ Yoshinori ISHIDO,² Loren W. ACTON,³ Keith T. STRONG,³ Tadashi HIRAYAMA,¹ Yutaka UCHIDA,⁴ Alan H. MCALLISTER,⁴ Ryoji MATSUMOTO,⁵ Saku TSUNETA,⁶ Toshifumi SHIMIZU,⁶ Hirohisa HARA,⁶ Takashi SAKURAI,¹ Kiyoshi ICHIMOTO,¹ Yohei NISHINO,¹ and Yoshiaki OGAWARA⁷

¹ National Astronomical Observatory, Mitaka, Tokyo 181

² Department of Physics and Astronomy, Aichi University of Education, Kariya, Aichi 448

³ Lockheed Palo Alto Research Laboratory, Palo Alto, CA 94304, U.S.A.

⁴ Department of Astronomy, Faculty of Science, The University of Tokyo, Bunkyo-ku, Tokyo 113

⁵ College of Arts and Sciences, Chiba University, Chiba, Chiba 260

⁶ Institute of Astronomy, The University of Tokyo, Mitaka, Tokyo 181

⁷ Institute of Space and Astronautical Science, Yoshinodai 3-chome, Sagami-hara, Kanagawa 229

(Received 1992 May 29; accepted 1992 June 26)

Abstract

Time series of Soft X-ray Telescope images have revealed many X-ray jets in the solar corona. The typical size of a jet is 5×10^3 – 4×10^5 km, the translational velocity is 30–300 km s^{−1}, and the corresponding kinetic energy is estimated to be 10^{25} – 10^{28} erg. Many of the jets are associated with flares in X-ray bright points, emerging flux regions, or active regions. They sometimes occur several times from the same X-ray feature. In some cases, a dark void appears after ejection at the footpoint of the jet. The void seems to be the result of a change in the topology of the X-ray emitting plasma, perhaps due to magnetic reconnection. Some jets show a structure which suggests a helical magnetic field configuration along the jet. One of the jets associated with a flaring bright point was identified as being an H α surge. In this case, the X-ray bright point is situated just on the H α bright point at the footpoint of the surge. The top of the surge is not bright in X-rays. We briefly discuss the origin of these newly discovered X-ray jets.

Key words: Sun: corona — Sun: X-rays — Sun: magnetic fields — Coronal jets

1. Introduction

There are many kinds of jet phenomena in the solar atmosphere, such as spicules (e.g., Beckers 1972), surges (e.g., Roy 1973), sprays (e.g., Tandberg-Hansen et al. 1980), and EUV jets (Brueckner and Bartoe 1983). Some jets (spicules and EUV jets) might be related to chromospheric and/or coronal heating; others (surges and sprays) often occur in association with flares. Furthermore, some of the solar jets (Shibata and Uchida 1986; Kurokawa et al. 1987) show common characteristics with astrophysical jets, such as bipolar molecular flows ejected from star-forming regions (Uchida and Shibata 1985). Hence, an understanding of the origin and structure of solar jets is important not only for solar physics, itself, but also for astrophysics in general.

The Soft X-ray Telescope (SXT) on Yohkoh (Tsuneta et al. 1991) has revealed many jet-like features, i.e., a transitory X-ray enhancements with an apparent collimated motion. It seems likely that their motion was a real flow of plasma, as indicated by the example of an X-ray jet associated with an H α surge. However, no Doppler shifts have yet been detected that can be directly

linked to them. In this letter we report on the discovery of such X-ray jets using data from the SXT, and discuss their origin.

2. Observations

We first found jets in the full-frame images (FFI) of SXT and, in a comprehensive survey of the data from 1991 November, discovered more than 20 jets there. The spatial resolution of FFI images is either half resolution ($\sim 5''$) or quarter resolution ($\sim 10''$). The time resolution ranges from a few minutes to an hour.

The typical size of a jet is 5×10^3 – 4×10^5 km, the translational velocity is 30–300 km s^{−1}, and the corresponding kinetic energy is about 10^{25} – 10^{28} erg. Many of the X-ray jets are associated with flares in X-ray bright points (XBPs), emerging flux regions (EFRs), or active regions (ARs). In some cases, a void appears at the footpoint of the jet after ejection. An example of this class of jet was the event of 1991 November 12 between 1128 and 1300 UT which occurred in NOAA 6918. There is another class of jet which shows meandering or undulat-

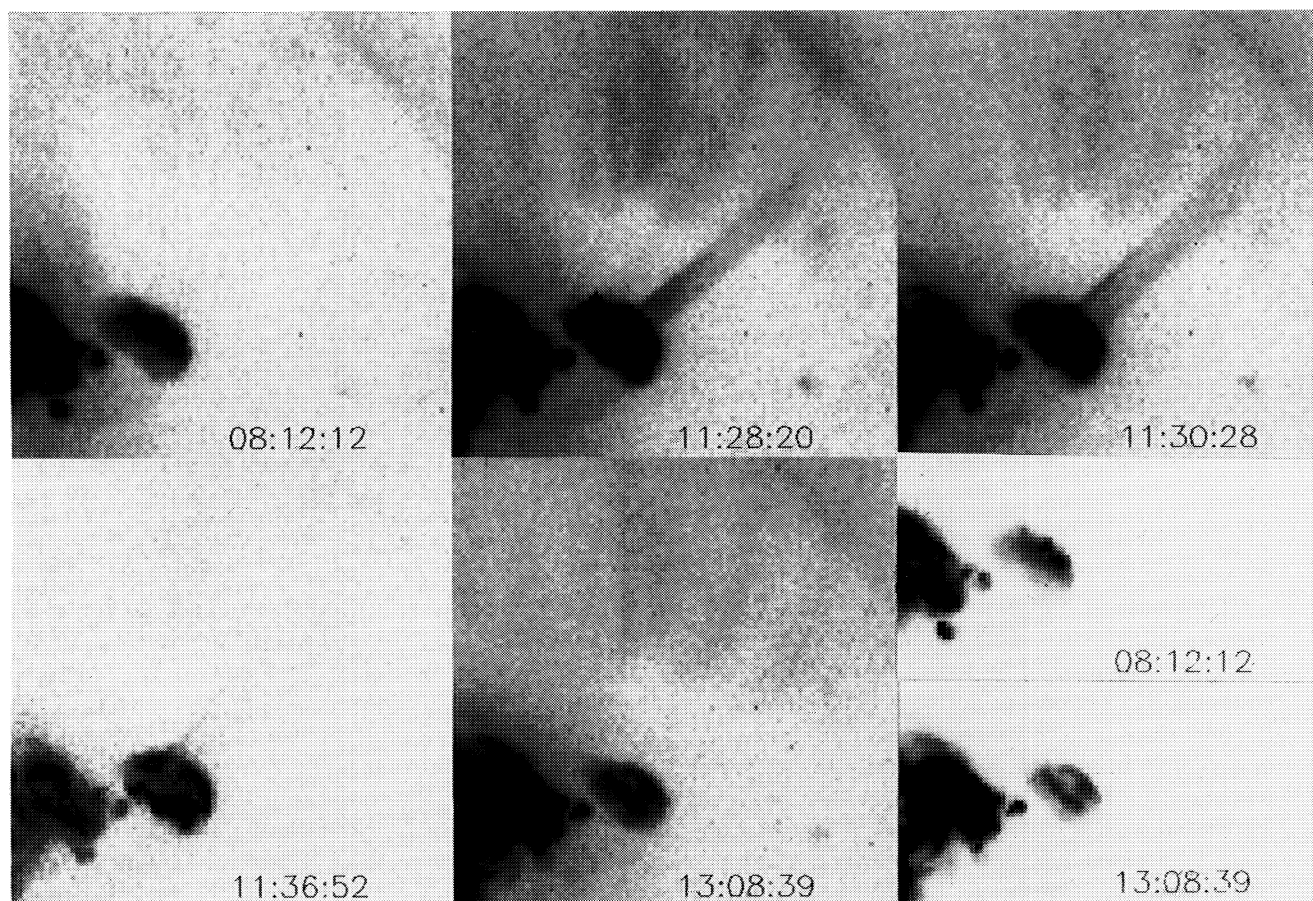


Fig. 1. Typical example of the X-ray jet observed by SXT at 0812–1315 UT on 1991 November 12, in active region NOAA 6918. These images were extracted from full-frame images of the Sun at the half-resolution mode; the pixel size is $\sim 5''$ (3500 km). The filter and the exposure time for each image are 081212 (Al/Mg/Mn, 2668 ms), 112820 (Al 0.1 μ , 2668 s), 113028 (Al/Mg/Mn, 2668 ms), 113652 (Al/Mg/Mn, 78 ms), 130839 (Al/Mg/Mn, 2668 ms). The size of each image is 100×100 pixels, i.e., 3.5×10^5 km \times 3.5×10^5 km. After ejection of the jet, a dark void appeared at the footpoint of the jet. See the last frame for comparison of pre-jet and post-jet images.

ing structure, suggesting a helical magnetic field configuration, such as the event of 1991 November 8 at 0313–0438 UT. We have not yet checked whether these are associated with optical jets, such as surges or sprays.

To improve the spatial and temporal resolution of X-ray partial frame images (PFI), images were used which are generally taken with $2''.45$ pixels and have a cadence of about 30 s. We found a small jet just south of the 1992 February 25 flare site in NOAA 7070 at 0145–0147 UT. The Flare Telescope at Mitaka (Sakurai et al. 1992) observed this event; it has become clear that this small X-ray jet was associated with an $H\alpha$ surge. We shall discuss these three classes of jets in the following section.

3. Results

3.1. Jets from Flaring ARs (or EFRs or BPs)

Figure 1 shows an example of a jet ejected from a flaring active region. It was observed in NOAA 6918 on 1991 November 12 between 0812 and 1315 UT. The jet first appeared at 112820 UT, and then disappeared at 130839 UT. The length of the jet, defined as the distance from the base to where its flux drops below 50 DN (for 2668 ms with Al/Mg/Mn filter), was about 2×10^5 km. (DN is defined as $\simeq 330$ eV of energy collected within a CCD pixel.) The lower limit of the velocity of the jet is ~ 100 km s^{-1} .

Interestingly, a void appeared at the footpoint of the jet after its ejection during 1136–1315 UT. It seems that there was less hot or dense plasma in the void. A similar void structure was also seen in other jets, such as the jets

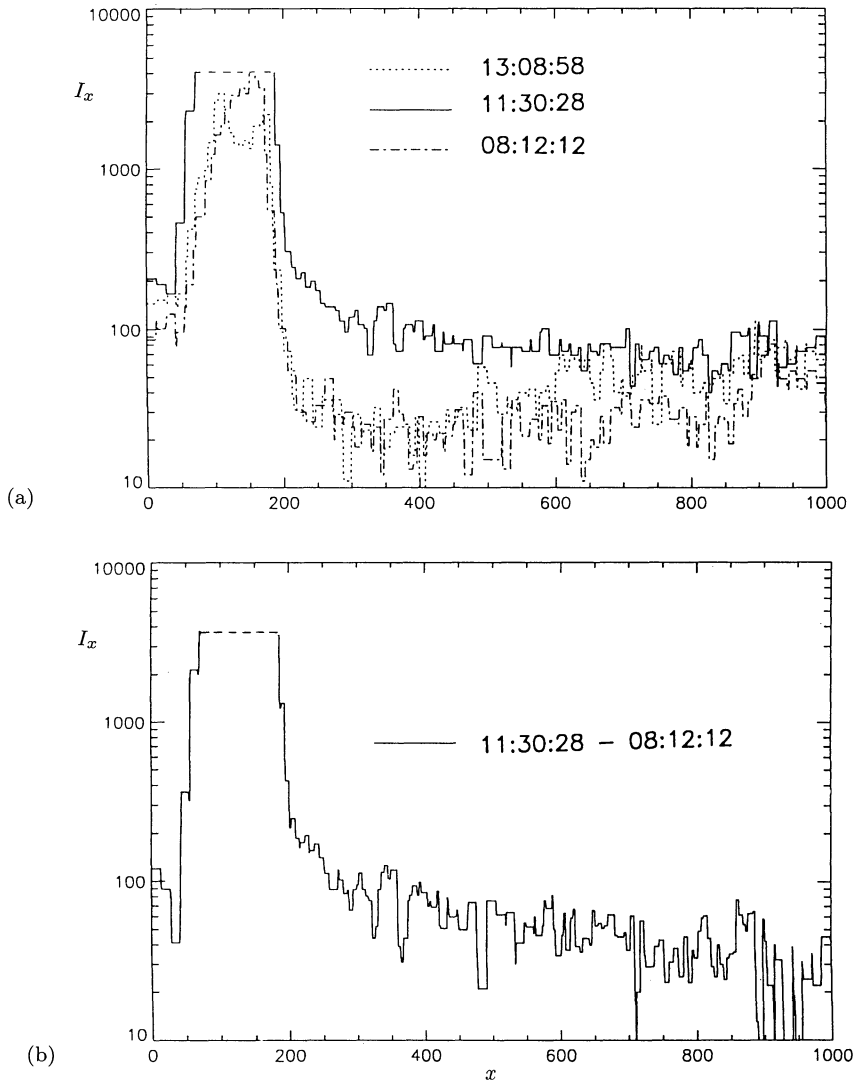


Fig. 2. (a) Intensity (DN) distribution along the jet at three different stages: pre-jet (081212), jet (113028), post-jet (130858), taken by the filter Al/Mg/Mn with 2668 ms at half resolution. The void is also seen in the AR at the footpoint of the jet (near $x = 150$). Note that the maximum intensity in the AR at 113028 is saturated. The unit of the distance (x) is $0.5''$. (b) Intensity of the jet itself; $I_x(\text{true jet}) = I_x(\text{jet}; 113028) - I_x(\text{pre-jet}; 081212)$. The saturated part is indicated by the dashed curve.

occurring on 1991 November 1, 1946 UT, and 1991 November 23, 0935 UT.

Another interesting feature of this jet is that its width was nearly constant. Since the potential field configuration of a magnetic bipole shows a strong divergence of the flux tube cross-sectional area, this observation needs explanation, especially since it is seen in many jets. It has also been noted by Klimchuk et al. (1992) that many coronal loops also seem to have constant cross sections.

A close examination of the jet morphology reveals that the northern side boundary moved slightly north between 112820 and 113652. The translational velocity was $20\text{--}30 \text{ km s}^{-1}$. If this is interpreted as being a new ejection

of plasma along the field lines just above the original jet, the velocity of the new ejection was about 1500 km s^{-1} .

Figure 2a shows the intensity distribution along the jet for three stages: pre-jet, jet, and post-jet stages. Figure 2b shows the intensity distribution of the jet, itself. The intensity rapidly decreases with distance from the AR at the footpoint of the jet. It follows from figure 2b that the intensity scale height $H_I = (|dI_x/dx|/I_x)^{-1} \sim 4 \times 10^4 \text{ km}$ near the AR ($200 < x < 400$), while $H_I \sim 2.3 \times 10^5 \text{ km}$ far from the AR ($x > 400$).

A preliminary study by the filter ratio method (Hara et al. 1992) with Al $0.1 \mu\text{m}$ and Al/Mg/Mn filters showed that the average temperature in the jet and in the ambi-



Fig. 3. Meandering or undulating jet observed at 031319–043839 UT on 1991 November 8. These images suggest the presence of a helical magnetic field along the jet. The size of each image is $950'' \times 1100''$ ($665000 \text{ km} \times 770000 \text{ km}$). These images are from the full-frame images taken at quarter resolution and exposure time 668 ms with an Al $0.1 \mu\text{m}$ filter.

ent corona was nearly the same, $\sim 3 \times 10^6 \text{ K}$. Hence, the high X-ray intensity in the jet region can be attributed to an increase in the density, not to an increase in the temperature. This, in turn, leads to the conclusion that the jet mass should be provided from somewhere, possibly from the footpoint of the jet in the chromosphere.

Since the emission measure (EM) is $= N_e^2 d \sim 4 \times 10^{26} \text{ cm}^{-5}$ for $T = 3 \times 10^6 \text{ K}$ and $\text{DN} = 100$ in the case of figure 2, we find that the electron densities at the footpoint ($\text{DN} = 4000$) and the midpoint ($\text{DN} = 100$) of the jet are $N_e \sim 2 \times 10^9 \text{ cm}^{-3}$ and $4 \times 10^8 \text{ cm}^{-3}$, respectively. Here, we have assumed that the jet had a uniform width of $d \sim 20000 \text{ km}$. The total mass of the

jet and the mass contained in the AR before ejection of the jet (at 081212 UT) were nearly equal, $M_{\text{AR}} \approx M_{\text{jet}} \sim 2 \times 10^{13} \text{ g}$. However, the mass in the AR increased to about $4 \times 10^{13} \text{ g}$ during the ejection of the jet (at 113028 UT). Hence, the mass in the flaring AR and the associated jet must have been supplied from the chromosphere, via evaporation (Hirayama 1974), as a result of the flare-like heating in the AR. The total (internal) energy released in this flare-like heating was $E_{\text{int}} \sim (3/2)M_{\text{AR}}R_gT/\mu \sim 3 \times 10^{28} \text{ erg}$ if $T \sim 3 \times 10^6 \text{ K}$, where $\mu = 0.5$ is the mean molecular weight and R_g is the gas constant. This is much larger than the total kinetic energy of the jet, $E_k \sim (1/2)M_{\text{jet}}v^2 \sim 10^{27} \text{ erg}$.



Fig. 4. (a) $H\alpha$ images of the surge of 1992 February 25, 0145–0217 UT, observed by the Flare Telescope at Mitaka. (b) A jet identified as an $H\alpha$ surge, which occurred on 1992 February 25, 0145–0147, near the flare in NOAA 7070. These images were taken with partial frame image mode at full resolution ($\sim 2.5''$); exposure times and filters are 6.3 ms (014518, Al 0.1 μ), and 17 ms (014550 and 014654 UT, Al/Mg/Mn). The contour curves overlayed on the SXT image show white light intensity distribution of the photospheric sunspots taken by the aspect sensor of the SXT. The image size is 95×77 pixels, i.e., $238'' \times 193''$. The $H\alpha$ images are coaligned with the X-ray images within an error of $\sim 3''$.

3.2. Jets with Meandering or Undulating Structure

Figure 3 shows another class of the jet with meandering or undulating structure, which occurred on 1991 November 8. The jet first appeared in the 041023 UT FFI image. The increase in its length seems to stop after 0410 UT. The length was $\sim 4 \times 10^5$ km at 0410, so that the lower limit of the translational velocity of the jet between 0313 UT and 0410 UT is ~ 110 km s $^{-1}$. The jet shows a meandering or undulating configuration, which suggests that it may have been along helically twisted magnetic field lines. Although many of X-ray jets fade away within a few hours after their birth, this jet was seen until 0807 UT (i.e., the lifetime was 4 hr).

The emission measure of the jet at the midpoint is $EM \sim 2 \times 10^{27}$ cm $^{-5}$. If $T \sim 3 \times 10^6$ K and the width of the jet is $d \sim 2 \times 10^4$ km, then $N_e \sim 1 \times 10^9$ cm $^{-3}$, $M_{jet} \sim 4 \times 10^{13}$ g, $E_k \sim 2 \times 10^{27}$ erg, and $E_{int} \sim 2 \times 10^{28}$ erg.

One of the most interesting features of this class of jet is its recurrence. In fact, many jets appeared at nearly the same place as that of November 8, i.e., November 5, 1419–1609 event ($v \sim 60$ km s $^{-1}$), November 5, 2045–2117 event ($v \sim 50$ km s $^{-1}$), and November 6, 1035 event (velocity uncertain).

3.3. Jets Identified with an $H\alpha$ Surge

Figure 4 shows the X-ray and $H\alpha$ images of a jet identified with an $H\alpha$ surge. A comparison of these images has

revealed that the X-ray and $H\alpha$ brightenings occurred at the footpoint of the surge. The X-ray brightening could not be seen at 014518 UT, but the $H\alpha$ brightening and the surge ejection could be seen at 014516. The X-ray jet at 014654 UT was nearly cospatial with the $H\alpha$ surge at 014658 UT. The length of the X-ray jet was ~ 5000 km at maximum (014654) and the velocity was ~ 100 km s $^{-1}$. On the other hand, the length of the $H\alpha$ surge increased up to 45000 km at 021728 UT, and the average velocity was only ~ 30 km s $^{-1}$. Although there were no X-ray images after 0150 UT, we examined the X-ray images at around 0148 UT and found that only an X-ray bright point can be seen at the footpoint of the surge after 0147 and that there was no strong X-ray emission at the top of the surge.

If the temperature of the X-ray jet was 3×10^6 K, EM of the jet would become 2×10^{29} cm $^{-5}$. Since the jet width was ~ 2000 km, we found $N_e \sim 3 \times 10^{10}$ cm $^{-3}$, $M_{jet} \sim 6 \times 10^{11}$ g, and $E_k \sim 3 \times 10^{25}$ erg. If the density of $H\alpha$ surge was $\sim 10^{11}$ cm $^{-3}$, the mass and the kinetic energy of $H\alpha$ surge would become 10^{14} g and 10^{28} erg, respectively, both of which are much larger than those of the X-ray jet.

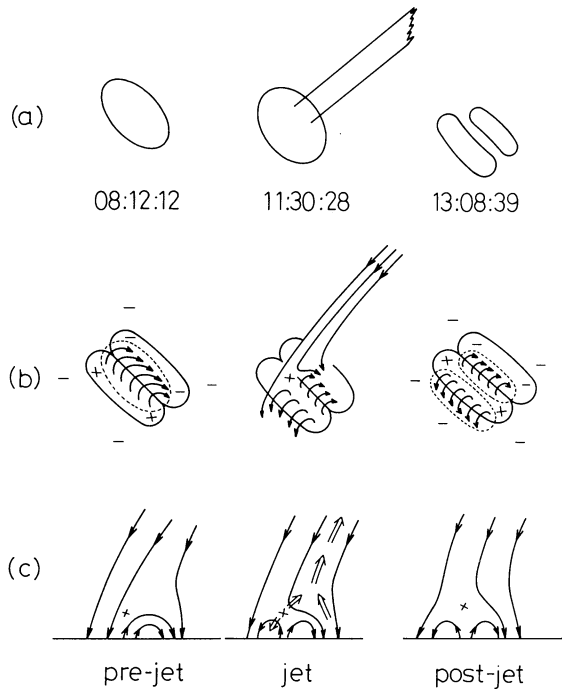


Fig. 5. Schematic picture of the possible physical situation of the 1991 November 12 jet. (a) Cartoons of the SXT image of the active regions and jets for pre-jet, jet, and post-jet stages. (b) Magnetogram data and the birds-eye view of the inferred magnetic field line configuration. (c) Side view of the magnetic reconnection occurring between the emerging flux and the pre-existing coronal field.

4. Discussion

What are the possible origins of the X-ray jets described above?

4.1. Evaporation Flow Resulting from a Rapid Energy Release by Magnetic Reconnection

Figure 5 is a schematic illustration summarizing our view of the November 12 jet. We suggest that the void seen after ejection of the jet is a true void (lack of hot or dense plasmas) and may be observational evidence of magnetic reconnection which occurred between the emerging flux and the pre-existing coronal field. This scenario is supported by the magnetogram data in the Solar Geophysical Data, and by the exact co-alignment of the two parts of the last frame of figure 1, which clearly shows that the second bright region (in the post-jet image) appears to the south of the first (in the pre-jet image), as expected from figure 5. The apparent constancy of the width of the jet may also be related to the magnetic reconnection, since in the geometry (with a magnetic neutral point) shown in figure 5, the magnetic field does not diverge as the dipole potential magnetic field

does.

From an emission measure analysis, it is concluded that the mass should come from the chromosphere, via evaporation. Hence, the basic physics seems to be essentially the same as those of the typical flares (Hirayama 1974). In fact, the active region at the footpoint of the jet was very bright in X-rays during ejection of the jet. The velocity of the evaporation flow as a result of the flare (e.g., Nagai 1984) amounted to $[2/(\gamma - 1)]C_s \simeq 3 \times C_s \simeq 1500(T/10^7\text{K})^{1/2} \text{ km s}^{-1}$ at maximum, where C_s is the sound speed of the flaring plasmas and $\gamma = 5/3$ is the specific heat ratio. The density decreased rapidly along the jet as shown in the intensity distribution in figure 2. An exact, self-similar solution for the one-dimensional flow expanding into vacuum shows that the density decreases as $\rho/\rho_0 = [1/(\gamma + 1)]^{2/(\gamma - 1)}[2 - (\gamma - 1)\xi]^{2/(\gamma - 1)}$, where ρ_0 is the mass density of the flaring plasmas and $\xi = x/(C_s t)$ is the similarity variable (e.g., Landau and Lifshitz 1959). This density distribution is not inconsistent with the observed intensity distribution near the AR ($200 < x < 400$ in figure 2). The apparent velocity of the iso-density (iso-intensity) surface of the jet becomes $v = [1/(\gamma - 1)][2 - (\gamma + 1)(\rho/\rho_0)^{(\gamma - 1)/2}]C_s = [3 - 4(\rho/\rho_0)^{1/3}]C_s \sim 30\text{--}350 \text{ km s}^{-1}$ if $C_s \simeq 500 \text{ km s}^{-1}$ and $\rho/\rho_0 = 0.2\text{--}0.4$, which explains the translational velocities of many X-ray jets. On the other hand, the very high velocity inferred from the change in the jet's width may be explained by the maximum velocity ($\sim 1500 \text{ km s}^{-1}$) or by the Alfvén speed ($V_A \simeq 1 - 3 \times 10^3 \text{ km s}^{-1}$).

Large-scale loop brightenings which are often observed in FFI images seem to be physically similar to this class of jets; they may be produced by evaporation flow as a result of magnetic reconnection occurring between two *closed* loops. If one of two loops is a very long loop, the evaporation flow would be observed as an X-ray jet.

4.2. Magnetic Twist

The meandering or undulating configuration of the November 8 jet suggests that the jet may have had a helically twisted magnetic field structure. It could thus be that the jet was accelerated by the $\mathbf{J} \times \mathbf{B}$ force when the nonlinear magnetic twist relaxed and propagated along the global flux tube (Shibata and Uchida 1986). Such a *magnetic twist jet* is produced when magnetic reconnection occurs between twisted and untwisted magnetic flux tubes. In this case, the maximum velocity (Shibata et al. 1990) would be $\sim 2 \times V_A \sim 2 \times 10^3(B/10\text{G})(N_e/10^9 \text{ cm}^{-3})^{-1/2} \text{ km s}^{-1}$. As for the propagation of the iso-density (iso-intensity) surface, the discussion above regarding evaporation flow also applies to a magnetic twist jet. The translational velocities of this kind of jet thus seem to be consistent with the magnetic-twist-jet model.

4.3. Reconnection with Mixed Hot and Cold Plasmas

It has long been discussed that the surges are usually not associated with X-ray emission, except for a few rare cases (Schmahl 1981; Svestka et al. 1990). This result, however, was strongly biased by the insensitivity of the X-ray sensors used for the comparisons. The discovery of a coexistence of the X-ray emission and $H\alpha$ emission in the surge places a strong constraint on the theory of surges. That is, the simple picture of pure hydrodynamic acceleration along a rigid magnetic flux tube (e.g., Steinolfson et al. 1979; Shibata et al. 1982) seems no longer to be valid for this class of surge. This is because if we input energy to the upper chromosphere to create an X-ray emitting plasma, the overlying cold plasma would be heated and would start to emit X-rays (i.e., evaporate), so that there would be no cold plasma jet emitting/absorbing $H\alpha$ (Sterling et al. 1991, 1992).

To make both hot and cold plasmas, we must assume a multi-dimensional magnetic field structure. Shibata et al. (1992) showed that a mixture of hot and cold plasmas is ejected along the current sheet as the result of magnetic reconnection between emerging flux and pre-existing coronal fields. In their model, cold plasmas are confined within magnetic islands as in the melon-seed spicule model of Uchida (1969). Thus, cold plasmas survive even if a huge amount of energy is released during the reconnection process. In a three-dimensional situation, the islands correspond to helically twisted field lines. Hence, the ejection of magnetic islands may be observed as an ejection of helical loops. In this sense, some of the surges may be a miniature version of eruptive prominences.

The Yohkoh mission has been realized through the efforts of many people, to whom we express our appreciation. We would also like to thank Drs. H. Hudson, A. C. Sterling, J. T. Mariska, and N. Nitta for helpful discussion. The Solar Flare Telescope Project was supported by a grant-in-aid from the Ministry of Education, Science and Culture (No. 63065001). LWA and KTS were supported by NASA contract NAS8-37334 with MSFC and by the Lockheed Independent Research Programme.

References

- Beckers, J. M. 1972, *Ann. Rev. Astron. Astrophys.*, **10**, 73.
 Brueckner, G., and Bartoe, J.-D. F. 1983, *Astrophys. J.*, **272**, 329.
 Hara, H., Tsuneta, S., Lemen, J. R., Acton, L. W., and McKiernan, J. M. 1992, *Publ. Astron. Soc. Japan*, **44**, L135.
 Hirayama, T. 1974, *Solar Phys.*, **34**, 323.
 Klimchuck, J. A., Lemen, J. R., Feldman, U., Tsuneta, S., and Uchida, Y. 1992, *Publ. Astron. Soc. Japan*, **44**, L181.
 Kurokawa, H., Hanaoka, Y., Shibata, K., and Uchida, Y. 1987, *Solar Phys.*, **108**, 251.
 Landau, L. D., and Lifshitz, E. M. 1959, *Fluid Mechanics*, (Pergamon Press, London), p. 353.
 Nagai, F. 1984, *Astrophys. J.*, **277**, 379.
 Roy, J.-R. 1973, *Solar Phys.*, **32**, 139.
 Sakurai, T., Ichimoto, K., Hiei, E., Irie, M., Kumagai, K., Miyashita, M., Nishino, Y., Yamaguchi, K., Fang, G., Kambry, M. A., Zhao, Z. W., and Shinoda, K. 1992, *Publ. Astron. Soc. Japan*, **44**, L7.
 Schmahl, E. J. 1981, *Solar Phys.*, **69**, 135.
 Shibata, K., Nishikawa, T., Kitai, R., and Suematsu, Y. 1982, *Solar Phys.*, **77**, 121.
 Shibata, K., Nozawa, S., and Matsumoto, R. 1992, *Publ. Astron. Soc. Japan*, **44**, 265.
 Shibata, K., Tajima, T., and Matsumoto, R. 1990, *Phys. Fluids B*, **2**, 1989.
 Shibata, K., and Uchida, Y. 1986, *Solar Phys.*, **103**, 299.
 Steinolfson, R. S., Schmahl, E. J., and Wu, S. T. 1979, *Solar Phys.*, **63**, 187.
 Sterling, A. C., Mariska, J. T., Shibata, K., and Suematsu, Y. 1991, *Astrophys. J.*, **381**, 313.
 Sterling, A. C., Shibata, K., and Mariska, J. T. 1992, submitted to *Astrophys. J.*
 Svestka, Z., Farnik, F., and Tang, F. 1990, *Solar Phys.*, **127**, 149.
 Tandberg-Hanssen, E., Martin, S. F., and Hansen, R. T. 1980, *Solar Phys.*, **65**, 357.
 Tsuneta, S., Acton, L., Bruner, M., Lemen, J., Brown, W., Carvalho, R., Catura, R., Freeland, S., Jurcevich, B., Morrison, M., Ogawara, Y., Hirayama, T., and Owens, J. 1991, *Solar Phys.*, **136**, 37.
 Uchida, Y. 1969, *Publ. Astron. Soc. Japan*, **21**, 128.
 Uchida, Y., and Shibata, K. 1985, *Publ. Astron. Soc. Japan*, **37**, 515.